Organometallic Macrocyclic Chemistry: Synthesis of Cationic Half-sandwich Iridium(I) Complexes of 1,4,7-Trithiacyclononane ([9]aneS$_3$). Crystal Structures of [Ir([9]aneS$_3$)(C$_2$H$_4$)$_2$]PF$_6$, [Ir([9]aneS$_3$)(C$_8$H$_{12}$)]PF$_6$ and [Ir([9]aneS$_3$)(C$_4$H$_6$)]PF$_6$·0.5Et$_2$O†

Alexander J. Blake, Malcolm A. Halcrow and Martin Schröder*
Department of Chemistry, The University of Edinburgh, West Mains Road, Edinburgh EH9 3JJ, UK

Reaction of [Ir$_2$L$_4$Cl$_2$] (L = C$_8$H$_{14}$ or 0.5C$_8$H$_{12}$) or [IrL$_4$Cl] (L = C$_2$H$_4$ or 0.5C$_4$H$_6$) with 1 molar equivalent of 1,4,7-trithiacyclononane ([9]aneS$_3$) and NH$_4$PF$_6$ in acetone, tetrahydrofuran or CH$_2$Cl$_2$ under N$_2$ at 293 K afforded the complexes [Ir([9]aneS$_3$)L$_2$]PF$_6$. The single-crystal structures of [Ir([9]aneS$_3$)(C$_2$H$_4$)$_2$]PF$_6$ and [Ir([9]aneS$_3$)(C$_8$H$_{12}$)]PF$_6$ have been determined and show that the complex cations adopt distorted five-co-ordinate geometries. For [Ir([9]aneS$_3$)(C$_2$H$_4$)$_2$]PF$_6$, Ir–S(1) 2.317(2), Ir–S(4) 2.402(2), Ir–S(7) 2.384(2), Ir–C(11) 2.173(9), Ir–C(12) 2.194(10), Ir–C(13) 2.146(8), Ir–C(14) 2.118(7), C(11)=C(12) 1.366(13) and C(13)=C(14) 1.443(11) Å. For [Ir([9]aneS$_3$)(C$_8$H$_{12}$)]PF$_6$, Ir–S(1) 2.319(5), Ir–S(4) 2.343(4), Ir–S(7) 2.419(4), Ir–C(11) 2.166(14), Ir–C(12) 2.199(14), Ir–C(15) 2.188(15), Ir–C(16) 2.141(15), C(11)=C(12) 1.411(19) and C(15)=C(16) 1.418(21) Å. The single-crystal structure of [Ir([9]aneS$_3$)(C$_4$H$_6$)]PF$_6$·0.5Et$_2$O shows this complex to have a five-co-ordinate stereochemistry analogous to that adopted by [Fe(CO)$_3$(C$_4$H$_6$)] with Ir–S(1) 2.321(2), Ir–S(4) 2.331(2), Ir–S(7) 2.325(2), Ir–C(11) 2.149(9), Ir–C(12) 2.141(9), Ir–C(13) 2.146(9), Ir–C(14) 2.115(10), C(11)=C(12) 1.433(13), C(12)–C(13) 1.381(13) and C(13)=C(14) 1.461(14) Å. Variable-temperature ^{1}H and ^{13}C NMR spectroscopic data on [M([9]aneS$_3$)(C$_2$H$_4$)$_2$]$^+$ and [M([9]aneS$_3$)(C$_4$H$_6$)]$^+$ (M = Rh or Ir) are consistent with the highly electrophilic character of the cationic fragments [M([9]aneS$_3$)]$^+$. On the basis of J(C–H) coupling data and of an analysis of bond-length distributions and observed dihedral angles in the complex, the butadiene ligand in [Ir([9]aneS$_3$)(C$_4$H$_6$)]$^+$ is assigned as η^4 bonded but with a significant σ^2 component.

There is intense current interest in the organometallic chemistry of rhodium and iridium with the cyclopentadienyl and pentamethylcyclopentadienyl anions.[1–3] Complexes of Rh and Ir with related six-electron donor ligands such as hydridotris(pyrazolyl)borate HB(pz)$_3$ and its per methylated analogue HB(Me$_3$C$_3$N$_2$)$_3$, [C{CH$_2$P(O)Ph$_2$}$_3$]$^-$, P$_3$O$_9$$^{3-}$ and MeC(CH$_2$PPh$_2$)$_3$ (tdpme) have also been well studied, with each protecting group imposing a different reactivity on the metal centres.[4–8] For example, the complexes [Rh{HB(Me$_3$C$_3$N$_2$)$_3$}L$_2$] (L = CO or C$_2$H$_4$) have been shown to undergo oxidative-addition reactions across aryl, vinyl and alkyl C–H bonds under mild thermal conditions,[4] while [Ir{C[CH$_2$P(O)Ph$_2$]$_3$}L$_2$] (L = CO or C$_2$H$_4$) catalyses the stereoselective hydrosilylation of alkynes.[8] The small-ring trithia macrocycle [9]aneS$_3$ (1,4,7-trithiacyclononane) is known to co-ordinate in a facial manner to a range of metal centres within the triads of Fe, Co, Ni, Cu and Zn.[9–11] We argued that [9]aneS$_3$ could also act as a protecting group analogous to [C$_5$H$_5$]$^-$, and were interested in what type of reactivity the half-sandwich complexes of Rh^I and Ir^I of this ligand might exhibit. This paper describes the synthesis and structures of a range of alkene iridium(I) complexes of [9]aneS$_3$; the synthesis and characterisation of the rhodium analogues [Rh([9]aneS$_3$)L$_2$]$^+$ (L = alkene, CO or phosphine) will be reported separately.

Very few iridium complexes of thioether ligands have been reported. Reaction of [Ir$_2$(C$_8$H$_{12}$)$_2$Cl$_2$] (C$_8$H$_{12}$ = cyclooctа-1,5-diene) with dth (dth = 2,5-dithiahexane) or S(C$_2$H$_4$SPh)$_2$ affords the products [Ir(dth)(C$_8$H$_{12}$)Cl] and [Ir{S(C$_2$H$_4$SPh)$_2$}(C$_8$H$_{12}$)]Cl respectively.[12] We have structurally characterised the octahedral iridium(III) species [Ir([9]aneS$_3$)$_2$]$^{3+}$, [Ir([9]aneS$_3$)$_2$H]$^{2+}$ [11] and *cis*-[Ir([14]aneS$_4$)Cl$_2$]$^+$ ([14]aneS$_4$ = 1,4,8,11-tetrathiacyclotetradecane).[13] No iridium(I) complexes of crown thioether ligands have been published to date, however, and there was therefore additional interest in determining the manner in which [9]aneS$_3$ might co-ordinate to this metal centre: [9]aneS$_3$ complexes of the d^8 metal ions Pd^{II}, Pt^{II} and Au^{III} exhibit quasi-five- or -six-co-ordinate geometries, with lengthened M···S apical interactions of 2.6–3.2 Å.[14] A preliminary communication of this work has appeared.[15]

Results and Discussion

Reaction of [Ir$_2$L$_4$Cl$_2$] [L = C$_8$H$_{14}$ (cyclooctene) or 0.5C$_8$H$_{12}$][16] or *in situ* generated solutions of [Ir(C$_2$H$_4$)$_4$Cl][17,18] with 1 molar equivalent of [9]aneS$_3$ and NH$_4$PF$_6$ in acetone or tetrahydrofuran (thf) under N$_2$ at 293 K afforded yellow solutions, from which pale yellow air-stable solid products could be isolated on addition of Et$_2$O. Analytical data for these compounds are consistent with the formulation [Ir([9]aneS$_3$)L$_2$]PF$_6$ (L = C$_2$H$_4$, C$_8$H$_{14}$ or 0.5C$_8$H$_{12}$). Fast atom bombardment (FAB) mass spectrometry shows positive-ion peaks with the correct isotopic distributions corresponding to the complexes [Ir([9]aneS$_3$)L$_2$]$^+$. The complex [Ir([9]aneS$_3$)(C$_8$H$_{14}$)$_2$]$^+$ is stable indefinitely at 298 K in air in the solid state, and for about 2 d at 298 K under N$_2$ in MeNO$_2$ or MeCN solution. This contrasts with [Rh([9]aneS$_3$)(C$_8$H$_{14}$)$_2$]$^+$ which decomposes rapidly in solution above 250 K.[15]

The ^{1}H NMR spectra of the complexes exhibited multiplets

† *Supplementary data available:* see Instructions for Authors, *J. Chem. Soc., Dalton Trans.*, 1994, Issue 1, pp. xxiii–xxviii.

Table 1 Free energies of activation for alkene hydrogen exchange for selected ethene complexes

Compound	T_c/K	$\Delta G^{\ddagger}(T_c)$/ kJ mol^{-1}	Ref.
$[Rh([9]aneS_3)(C_2H_4)_2]^+$	< 175	< 33	20
$[Ir([9]aneS_3)(C_2H_4)_2]^+$	177	33.3	This work
$[Rh(C_5H_5)(C_2H_4)_2]$	328	64	1
$[Rh(C_5Me_5)(C_2H_4)_2]$	> 333	> 65	21
$[Rh(C_9H_7)(C_2H_4)_2]$	240	43	22
$[Ir(C_5Me_5)(C_2H_4)_2]$	> 383	> 80	23
$[Ir\{HB(pz)_3\}(C_2H_4)_2]$	263	54	5
$[Ir\{C[CH_2P(O)Ph_2]_3\}(C_2H_4)_2]$	< 298	< 58	8
$[Ru(C_6Me_6)(C_2H_4)_2]$	> 389	> 84	24
$[Os(CO)(NO)(PPh_3)(C_2H_4)]$	208	40	25
$[Pt(acac)(C_2H_4)Cl]$*	253	51	26
$[Pt(PPh_3)(C_2H_4)_2]$	225	42	27

* acac = Acetylacetonate.

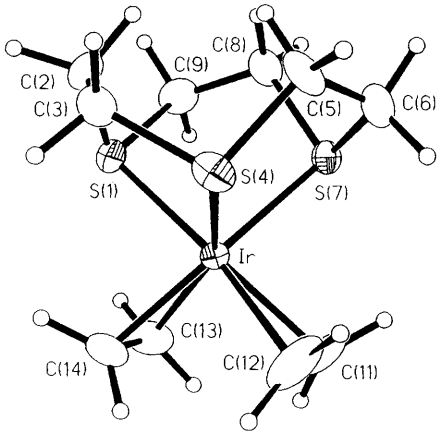

Fig. 1 View of $[Ir([9]aneS_3)(C_2H_4)_2]^+$ with the numbering scheme adopted

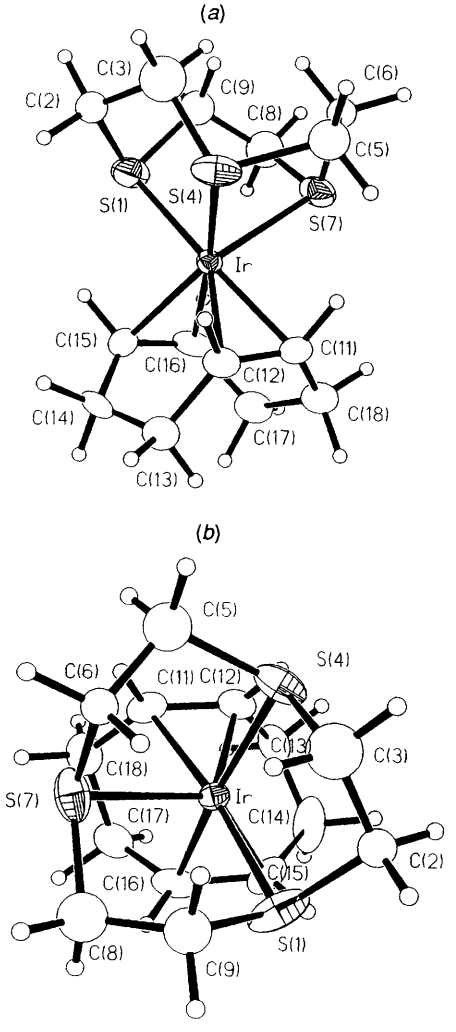

Fig. 2 Two views of $[Ir([9]aneS_3)(C_8H_{12})]^+$ with the numbering scheme adopted

centred near δ 3.04 (L = C_2H_4) and 2.6 (L = C_8H_{14} or $0.5C_8H_{12}$) arising from the $[9]aneS_3$ macrocycle, as well as peaks expected from the η^2-co-ordinated alkenes in integral ratios consistent with the formulation $[Ir([9]aneS_3)L_2]^+$. In addition to resonances for alkene ligands, ^{13}C DEPT (distortionless enhancements by polarisation transfer) NMR spectroscopy for all three complexes showed a single resonance in the range δ 35.2–35.6 from the $[9]aneS_3$ methylene centres, indicating that the macrocyclic C atoms are equivalent in solution. This type of equilibration has been noted previously for $[9]aneS_3$ complexes of non-d^6 metal ions.[19] No evidence in favour of structures involving σ- or η^3-co-ordinated alkenes was observed, in contrast to the products obtained from similar reactions using hydrido(pyrazolyl)borate ligands.[5] No reaction was observed between $[Ir([9]aneS_3)L_2]^+$ (L = C_2H_4 or C_8H_{14}) and CO or C_8H_{12} in thf or CH_2Cl_2 solutions at 293 K or under reflux, consistent with a five-co-ordinate, 18-electron configuration for these complexes in solution.[1]

The ^1H NMR spectrum of $[Ir([9]aneS_3)(C_2H_4)_2]PF_6$ in $(CD_3)_2CO$ at 293 K exhibited a multiplet at δ 3.11–2.98 corresponding to the SCH_2 protons of the co-ordinated macrocycle, and a singlet at δ 2.19 from the ethene H atoms. A variable-temperature ^1H NMR study (360.13 MHz) in 2:1 CD_2Cl_2–$[^2H_8]$thf allowed the measurement of T_c for exchange of the ethene H atoms as 177 ± 1 K: below this temperature, two new resonances corresponding to the outer and inner ethene proton environments were observed at δ 2.57 and *ca.* 1.89 (partially obscured by a solvent peak). These data correspond to a calculated activation energy of $\Delta G^{\ddagger}$ = 33.3 ± 0.2 kJ mol^{-1} at this temperature. This compares with the value found for $[Rh([9]aneS_3)(C_2H_4)_2]^+$, where T_c for ethene rotation was below 175 K.[20] No decoalescence of the ^1H NMR resonance due to the $[9]aneS_3$ ligand in $[Ir([9]aneS_3)(C_2H_4)_2]PF_6$ was observed down to 158 K.

Given the observed inactivity of $[M([9]aneS_3)(C_2H_4)_2]^+$ (M = Rh or Ir) towards nucleophilic substitution reactions, the most likely mechanism of ethene hydrogen exchange in these compounds is rotation of the co-ordinated ethene ligands about the metal–alkene σ-bond axis. Activation energies for ethene rotation of ≤33.3 kJ mol^{-1} are substantially lower than for related ethene complexes of Rh^I or Ir^I (Table 1): this implies that M→C_2H_4 π-back donation is relatively weak in $[M([9]aneS_3)(C_2H_4)_2]^+$, and hence the fragments $[M([9]aneS_3)]^+$ (M = Rh or Ir) contain unusually electrophilic rhodium(I) and iridium(I) centres. This is consistent with the potential π-acceptor ability of $[9]aneS_3$,[9,10,28] and the overall +1 charge on these cationic complexes.

In order to quantify further the iridium–alkene bonding in the complexes $[Ir([9]aneS_3)L_2]^+$ and to ascertain the co-ordination geometries adopted by these species, single-crystal X-ray analyses of $[Ir([9]aneS_3)(C_2H_4)_2]PF_6$ and $[Ir([9]aneS_3)(C_8H_{12})]PF_6$ were undertaken. Single crystals were obtained by diffusion of Et_2O vapour into acetone solutions of the complexes. Figs. 1 and 2 give views of the two complex cations, and bond lengths, angles and torsion angles are listed in Tables 2 and 3.

The single-crystal structure of $[Ir([9]aneS_3)(C_2H_4)_2]PF_6$

Table 2 Bond lengths (Å), angles and torsion angles (°) with standard deviations for $[Ir([9]aneS_3)(C_2H_4)_2]^+$

Ir–S(1)	2.317(2)	C(2)–C(3)	1.505(10)
Ir–S(4)	2.402(2)	C(3)–S(4)	1.822(8)
Ir–S(7)	2.384(2)	S(4)–C(5)	1.842(7)
Ir–C(11)	2.173(9)	C(5)–C(6)	1.529(10)
Ir–C(12)	2.194(10)	C(6)–S(7)	1.812(7)
Ir–C(13)	2.146(8)	S(7)–C(8)	1.818(7)
Ir–C(14)	2.118(7)	C(8)–C(9)	1.524(10)
S(1)–C(2)	1.818(8)	C(11)–C(12)	1.366(13)
S(1)–C(9)	1.820(8)	C(13)–C(14)	1.443(11)
S(1)–Ir–S(4)	87.32(6)	C(13)–Ir–C(14)	39.5(3)
S(1)–Ir–S(7)	87.52(6)	Ir–S(1)–C(2)	106.7(2)
S(1)–Ir–C(11)	156.8(2)	Ir–S(1)–C(9)	102.2(2)
S(1)–Ir–C(12)	165.8(3)	C(2)–S(1)–C(9)	101.4(3)
S(1)–Ir–C(13)	83.56(21)	S(1)–C(2)–C(3)	112.6(5)
S(1)–Ir–C(14)	86.30(20)	C(2)–C(3)–S(4)	114.6(5)
S(4)–Ir–S(7)	86.30(6)	Ir–S(4)–C(3)	100.7(2)
S(4)–Ir–C(11)	113.5(2)	Ir–S(4)–C(5)	105.5(2)
S(4)–Ir–C(12)	83.9(3)	C(3)–S(4)–C(5)	101.2(3)
S(4)–Ir–C(13)	148.9(2)	S(4)–C(5)–C(6)	111.9(5)
S(4)–Ir–C(14)	110.4(2)	C(5)–C(6)–S(7)	114.2(5)
S(7)–Ir–C(11)	83.86(23)	Ir–S(7)–C(8)	103.1(2)
S(7)–Ir–C(12)	102.9(3)	Ir–S(7)–C(8)	104.8(2)
S(7)–Ir–C(13)	122.7(2)	C(6)–S(7)–C(8)	100.9(3)
S(7)–Ir–C(14)	161.9(2)	S(7)–C(8)–C(9)	111.3(5)
C(11)–Ir–C(12)	36.4(3)	S(1)–C(9)–C(8)	113.7(5)
C(11)–Ir–C(13)	83.1(3)	Ir–C(11)–C(12)	72.6(5)
C(11)–Ir–C(14)	95.3(3)	Ir–C(12)–C(11)	70.9(5)
C(12)–Ir–C(13)	98.4(3)	Ir–C(13)–C(14)	69.2(4)
C(12)–Ir–C(14)	86.4(3)	Ir–C(14)–C(13)	71.3(4)

C(9)–S(1)–C(2)–C(3)	−133.3(5)
C(2)–S(1)–C(9)–C(8)	64.4(6)
S(1)–C(2)–C(3)–S(4)	48.0(7)
C(2)–C(3)–S(4)–C(5)	65.5(6)
C(3)–S(4)–C(5)–C(6)	−132.9(5)
S(4)–C(5)–C(6)–S(7)	49.3(6)
C(5)–C(6)–S(7)–C(8)	64.3(5)
C(6)–S(7)–C(8)–C(9)	−135.3(5)
S(7)–C(8)–C(9)–S(1)	50.6(6)

shows (Fig. 1) five-co-ordination at Ir^I [Ir–S(1) 2.317(2), Ir–S(4) 2.402(2), Ir–S(7) 2.384(2); Ir–C(11) 2.173(9), Ir–C(12) 2.194(10), Ir–X(1) 2.073(9), Ir–C(13) 2.146(8), Ir–C(14) 2.118(7), Ir–X(2) 2.007(8), C(11)–C(12) 1.336(13) and C(13)–C(14) 1.443(11) Å], where X(1), X(2) are the midpoints of the C(11)=C(12) and C(13)=C(14) ethene double bonds respectively. By considering the internal angles at Ir, the stereochemistry can be best described as distorted trigonal bipyramidal with S(1) and C(11)=C(12) at apical sites. However, the constraints of the $[9]aneS_3$ macrocycle lead to highly distorted angles within the equatorial $S_2(C_2H_4)$ plane of the complex: S(1)–Ir–X(1) 173.9(2), S(1)–Ir–X(2) 84.6(2), S(4)–Ir–X(1) 98.8(2), S(4)–Ir–X(2) 129.9(2), S(7)–Ir–X(1) 93.6(2), S(7)–Ir–X(2) 142.3(3), X(1)–Ir–X(2) 90.9(3), S–Ir–S 86.30(6)–87.52(6)°. This geometry is very similar to the trigonal-bipyramidal stereochemistries observed in the analogous rhodium(I) species $[Rh([9]aneS_3)L_2]^+$ (L = C_2H_4 or $0.5C_8H_{12}$)[15,20] and $[Rh_2(C_8H_{12})_2([20]aneS_6)]^{2+}$ ($[20]aneS_6$ = 1,4,7,11,14,17-hexathiacycloicosane).[29] The Ir–C and intra-ethene C=C distances are similar to those observed in other iridium–ethene complexes, for example the trigonal-bipyramidal cation $[Ir(PMe_2Ph)_3(C_2H_4)_2]^+$ contains two equatorial C_2H_4 ligands, Ir–C 2.140(16)–2.171(15), C=C 1.401(25), 1.427(24) Å,[30] while for *trans*-$[Ir(PPh_3)_2(C_2H_4)Cl]$, Ir–C 2.123(8), 2.112(8), C=C 1.375(10) Å.[31] In $[Ir([9]aneS_3)(C_2H_4)_2]^+$ the axial Ir–S(1) bond is shorter than the equatorial Ir–S distances, as expected for a d^8 trigonal-bipyramidal complex.[32] However, the axial ethene ligand [C(11)=C(21)] is less closely bound to the metal centre than is the equatorial ethene [C(13)=C(14)] since the former is directly *trans* to the thioether S-donor S(1). The

Table 3 Bond lengths (Å), angles and torsion angles (°) with standard deviations for $[Ir([9]aneS_3)(C_8H_{12})]^+$

Ir–S(1)	2.319(5)	C(11)–C(18)	1.499(21)
Ir–S(4)	2.343(4)	C(12)–C(13)	1.528(21)
Ir–S(7)	2.419(4)	C(13)–C(14)	1.474(23)
Ir–C(11)	2.166(14)	C(14)–C(15)	1.482(23)
Ir–C(12)	2.199(14)	C(15)–C(16)	1.418(21)
Ir–C(15)	2.188(15)	C(16)–C(17)	1.566(21)
Ir–C(16)	2.141(15)	C(17)–C(18)	1.528(21)
C(11)–C(12)	1.411(19)		
S(1)–Ir–S(4)	86.35(15)	Ir–S(4)–C(3′)	102.3(5)
S(1)–Ir–S(7)	86.79(15)	Ir–S(4)–C(5)	100.6(4)
S(1)–Ir–C(11)	174.2(4)	Ir–S(4)–C(5′)	105.2(6)
S(1)–Ir–C(12)	147.5(4)	C(3)–S(4)–C(5)	102.0(7)
S(1)–Ir–C(15)	84.3(4)	C(3′)–S(4)–C(5′)	97.8(7)
S(1)–Ir–C(16)	95.3(4)	Ir–S(7)–C(6)	103.5(5)
S(4)–Ir–S(7)	85.99(14)	Ir–S(7)–C(6′)	100.6(5)
S(4)–Ir–C(11)	97.2(4)	Ir–S(7)–C(8)	98.8(5)
S(4)–Ir–C(12)	86.8(4)	Ir–S(7)–C(8′)	102.6(5)
S(4)–Ir–C(15)	134.5(4)	C(6)–S(7)–C(8)	105.8(7)
S(4)–Ir–C(16)	171.9(4)	C(6′)–S(7)–C(8′)	101.0(7)
S(7)–Ir–C(11)	88.9(4)	Ir–C(11)–C(12)	72.4(8)
S(7)–Ir–C(12)	124.3(4)	Ir–C(11)–C(18)	110.3(9)
S(7)–Ir–C(15)	137.6(4)	C(12)–C(11)–C(18)	124.8(13)
S(7)–Ir–C(16)	102.0(4)	Ir–C(12)–C(11)	69.9(8)
C(11)–Ir–C(12)	37.7(5)	Ir–C(12)–C(13)	114.3(9)
C(11)–Ir–C(15)	96.3(5)	C(11)–C(12)–C(13)	123.3(12)
C(11)–Ir–C(16)	81.8(5)	C(12)–C(13)–C(14)	111.4(13)
C(12)–Ir–C(15)	78.1(5)	C(13)–C(14)–C(15)	115.1(14)
C(12)–Ir–C(16)	87.6(5)	Ir–C(15)–C(14)	112.1(10)
C(15)–Ir–C(16)	38.2(6)	Ir–C(15)–C(16)	69.1(8)
Ir–S(1)–C(2)	103.6(5)	C(14)–C(15)–C(16)	123.9(14)
Ir–S(1)–C(2′)	106.0(6)	Ir–C(16)–C(15)	72.7(8)
Ir–S(1)–C(9)	105.1(5)	Ir–C(16)–C(17)	111.5(10)
Ir–S(1)–C(9′)	100.9(5)	C(15)–C(16)–C(17)	125.0(13)
C(2)–S(1)–C(9)	97.2(7)	C(16)–C(17)–C(18)	113.8(12)
C(2′)–S(1)–C(9′)	101.9(7)	C(11)–C(18)–C(17)	112.9(12)
Ir–S(4)–C(3)	105.2(5)		

C(9)–S(1)–C(2)–C(3)	−59.8(11)
C(2)–S(1)–C(9)–C(8)	142.8(10)
S(1)–C(2)–C(3)–S(4)	−56.6(11)
C(2)–C(3)–S(4)–C(5)	142.1(10)
C(3)–S(4)–C(5)–C(6)	−52.7(11)
S(4)–C(5)–C(6)–S(7)	−60.8(11)
C(5)–C(6)–S(7)–C(8)	137.3(10)
C(6)–S(7)–C(8)–C(9)	−54.1(11)
S(7)–C(8)–C(9)–S(1)	−61.4(12)
C(9′)–S(1)–C(2′)–C(3′)	−140.4(11)
C(2′)–S(1)–C(9′)–C(8′)	54.7(12)
S(1)–C(2′)–C(3′)–S(4)	56.7(12)
C(2′)–C(3′)–S(4)–C(5′)	57.9(12)
C(3′)–S(4)–C(5′)–C(6′)	−144.1(11)
S(4)–C(5′)–C(6′)–S(7)	60.8(12)
C(5′)–C(6′)–S(7)–C(8′)	55.0(12)
C(6′)–S(7)–C(8′)–C(9′)	−139.3(10)
S(7)–C(8′)–C(9′)–S(1)	61.4(12)
C(18)–C(11)–C(12)–C(13)	3.6(22)
C(12)–C(11)–C(18)–C(17)	47.7(19)
C(11)–C(12)–C(13)–C(14)	−96.3(17)
C(12)–C(13)–C(14)–C(15)	31.6(19)
C(13)–C(14)–C(15)–C(16)	45.9(21)
C(14)–C(15)–C(16)–C(17)	1.4(23)
C(15)–C(16)–C(17)–C(18)	−88.9(18)
C(16)–C(17)–C(18)–C(11)	26.6(17)

equatorial S-donors S(4) and S(7) are not directly *trans* to the equatorial ethene [C(13)=C(14)] and so no *trans* lengthening of the Ir–C(13) and Ir–C(14) linkages is observed. This pattern of metal–alkene bonding has also been observed in the related rhodium thioether complexes mentioned above, and in other trigonal-bipyramidal complexes of Rh^I and Ir^I with chelating alkenes such as $[Ir(PR_3)_2(C_8H_{12})Me]$ (PR_3 = PMe_2Ph, $0.5Ph_2PCH_2CH_2PPh_2$ or $0.5Ph_2PCH_2CH_2CH_2PPh_2$)[33] and

$[Rh\{(CF_3CO)_2CH\}L(C_5H_5N)]$ [L = 2,3-bis(methoxycarbonyl)bicyclo[2.2.1]hepta-2,5-diene].[34] Another possible explanation for the shortened Ir–C and lengthened C=C distances associated with C(13)–C(14) is the formation of a metallocyclopropane moiety. However, the low barrier to ethene rotation observed for $[Ir([9]aneS_3)(C_2H_4)_2]^+$ and the oxidation observed by cyclic voltammetry (see below) suggest more strongly that the complex may best be regarded as an iridium(I) bis(π-ethene) complex.

The single-crystal structure of $[Ir([9]aneS_3)(C_8H_{12})]PF_6$ also shows (Fig. 2) a five-co-ordinate complex cation [Ir–S(1) 2.319(5), Ir–S(4) 2.343(4), Ir–S(7) 2.419(4); Ir–C(11) 2.166(14), Ir–C(12) 2.199(14), Ir–X(1) 2.067(14), Ir–C(15) 2.188(15), Ir–C(16) 2.141(15), Ir–X(2) 2.045(15) Å], where X(1), X(2) are the midpoints of the C(11)=C(12) and C(15)=C(16) vectors respectively. However, the angles about the iridium are more consistent with a geometry midway between trigonal bipyramidal and square pyramidal [S(1)–Ir–X(1) 166.1(4), S(1)–Ir–X(2) 90.0(4), S(4)–Ir–X(1) 92.1(4), S(4)–Ir–X(2) 153.3(5), S(7)–Ir–X(1) 107.2(4), S(7)–Ir–X(2) 120.2(4), X(1)–Ir–X(2) 85.5(6)°]. As a result of this the C=C bond lengths C(11)–C(12) 1.411(19) and C(15)–C(16) 1.418(21) Å are more similar to one another than in trigonal-bipyramidal $[Ir([9]aneS_3)(C_2H_4)_2]PF_6$. Conversion of the observed structure for $[Ir([9]aneS_3)(C_8H_{12})]PF_6$ into a trigonal-bipyramidal geometry analogous to that observed for $[Ir([9]aneS_3)(C_2H_4)_2]^+$ involves rotation of the $[9]aneS_3$ macrocycle by some 11° about the central $Ir([9]aneS_3)$ C_3 axis, whilst rotation by −11° would give a square-pyramidal stereochemistry. The occurrence of different geometries for these two complexes is consistent with the fluxionality observed for $[Ir([9]aneS_3)(C_2H_4)_2]^+$ in solution (see above), and suggests that the detailed stereochemistries exhibited by $[Ir([9]aneS_3)L_2]^+$ (L = C_2H_4 or $0.5C_8H_{12}$) in the solid state may be influenced by crystal-packing forces.

Reaction of a solution of $[Ir(C_4H_6)_2Cl]$ generated *in situ*[18] with $[9]aneS_3$ and NH_4PF_6 in CH_2Cl_2 under identical conditions to those described above afforded a colourless microcrystalline product. Analytical data for this complex are consistent with the formulation $[Ir([9]aneS_3)(C_4H_6)]PF_6$, while FAB mass spectrometry shows positive-ion peaks with the correct isotopic distributions at m/z = 427, 399 and 372, corresponding to $[Ir([9]aneS_3)(C_4H_6)]^+$, $[Ir([9]aneS_3)(C_2H_2)]^+$ and $[Ir([9]aneS_3 - H)]^+$ respectively.

The ^1H NMR spectrum of $[Ir([9]aneS_3)(C_4H_6)]PF_6$ in $(CD_3)_2CO$ at 293 K shows multiplet resonances centred at δ 5.29, 2.25 and 0.43 arising from the butadiene ligand and at δ 3.08–2.72 from the $[9]aneS_3$ macrocycle. The ^{13}C NMR spectrum obtained under the same conditions exhibited peaks at δ 80.94 and 22.34 due to co-ordinated C_4H_6 and three peaks of equal intensity in the region expected for the $[9]aneS_3$ ligand at δ 37.63, 36.46 and 35.04 (Fig. 3). This shows that $[Ir([9]aneS_3)(C_4H_6)]^+$ has a static solution structure at 293 K with three distinct methylene environments for the $[9]aneS_3$ macrocycle, in contrast to the complexes $[Ir([9]aneS_3)L_2]^+$ (L = C_2H_4, C_8H_{14} or $0.5C_8H_{12}$) described above where only one resonance is observed for the carbon centres of the co-ordinated $[9]aneS_3$. It is well known that the activation barrier for scrambling of the CO ligands in $[Fe(CO)_3(1,3\text{-diene})]$ complexes by rotation of the $Fe(CO)_3$ fragment relative to the diene ligand is significantly higher than for analogous complexes of non-conjugated dienes.[35,36] For a relatively non-substitution-labile third-row metal complex such as $[Ir([9]aneS_3)(C_4H_6)]^+$ the barriers to rotation would be expected to be greater than those for first-row species. Indeed, the NMR data are consistent with $[Ir([9]aneS_3)(C_4H_6)]^+$ adopting a static, five-co-ordinate structure. In addition, significant $[Ir^I(\eta^4\text{-}C_4H_6)]^+ \longleftrightarrow [Ir^{III}(\sigma,\eta^2,\sigma\text{-}C_4H_6)]^+$ tautomerism of the type observed for 1,3-diene complexes of Hf, Ta and Zr[37–40] (see below) might inhibit fluxionality about the Ir, which would possess significant d^6 character. In order to examine the Ir–C_4H_6 bonding in this complex a single-crystal X-ray analysis of $[Ir([9]aneS_3)(C_4H_6)]PF_6$ was undertaken.

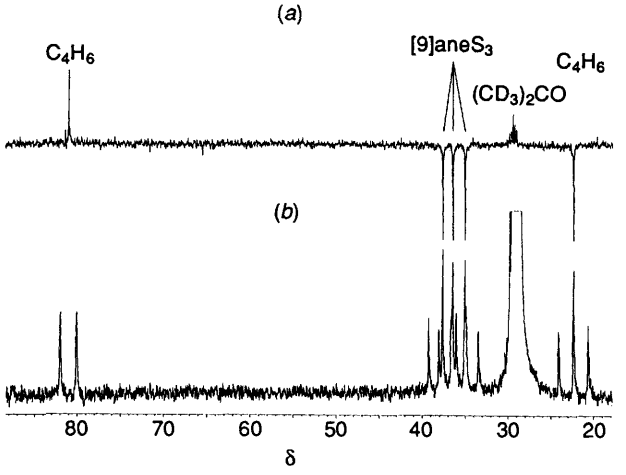

Fig. 3 The ^{13}C NMR spectra of $[Ir([9]aneS_3)(C_4H_6)]^+$ [90.56 MHz, $(CD_3)_2CO$, 293 K]: (*a*) DEPT, (*b*) broadband ^1H-coupled

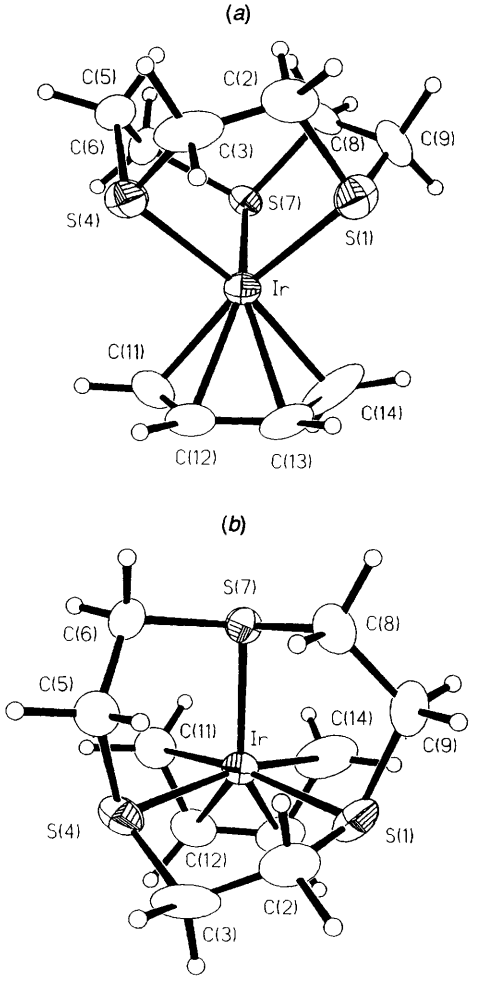

Fig. 4 Two views of $[Ir([9]aneS_3)(C_4H_6)]^+$ with the numbering scheme adopted

Diffusion of Et_2O vapour into an acetone solution of the complex afforded colourless tablets of composition $[Ir([9]aneS_3)(C_4H_6)]PF_6{\cdot}0.5Et_2O$. Two views of the complex cation are shown in Fig. 4, and selected bond lengths, angles and torsion angles are listed in Table 4. The structural analysis confirms a five-co-ordinate structure for $[Ir([9]aneS_3)(C_4H_6)]^+$ with Ir–S(1) 2.321(2), Ir–S(4) 2.331(2) and Ir–S(7) 2.325(2) Å.

The stereochemistry adopted by the complex is analogous to that observed for other five-co-ordinate d^8 butadiene complexes such as $[Fe(CO)_3(C_4H_6)]$[41] and $[Co(PMe_3)_3(C_4H_6)]^+$,[42] with one Ir–S bond [Ir–S(7)] situated over the open edge of the C_4H_6 ligand. Extended Hückel molecular-orbital (EHMO) calculations have shown that this orientation of a d^8 $[ML_3]^{n+}$ fragment relative to a C_4H_6 ligand is electronically favoured.[36] The butadiene ligand is bound to the Ir with Ir–C(11) 2.149(9), Ir–C(12) 2.141(9), Ir–C(13) 2.146(9), Ir–C(14) 2.115(10) Å, Ir–X(1) 2.022(9), Ir–X(2) 2.029(9), Ir–X(3) 2.002(9) Å, X(1)–Ir–S(1) 148.62(6), X(2)–Ir–S(1) 114.94(6), X(3)–Ir–S(1) 97.65(6), X(1)–Ir–S(4) 96.97(6), X(2)–Ir–S(4) 112.63(6), X(3)–Ir–S(4) 145.61(6), X(1)–Ir–S(7) 122.9(5), X(2)–Ir–S(7) 147.69(5) and X(3)–Ir–S(7) 124.88(5)°, where X(1), X(2) and X(3) are the midpoints of the C(11)–C(12), C(12)–C(13) and C(13)–C(14) linkages respectively. Importantly, the CH–CH bond distance is *shorter* than the CH_2=CH distance, C(11)–C(12) 1.433(13), C(12)–C(13) 1.381(13) and C(13)–C(14) 1.461(14) Å; for free butadiene C=C 1.343(1) and C–C 1.467(1) Å.[43] Whilst equalisation of the butadiene C–C bond lengths would be expected on co-ordination to a metal ion,[44] the degree of distortion observed for $[Ir([9]aneS_3)(C_4H_6)]^+$ is unusual for butadiene complexes of Groups VIII–X metals. This notwithstanding, the bond lengths are comparable with those found in $[Ir(C_4H_6)_2Cl]$, CH_2=CH 1.41(1) and CH–CH 1.47(1) Å.[45] The pattern of C_4H_6 C–C distances observed for $[Ir([9]aneS_3)(C_4H_6)]^+$ is however more typical of those found in butadiene complexes of early transition metals such as Hf, Ta and Zr, which are generally formulated as metallacyclopent-3-ene species:[38] for example for $[Ta(\eta\text{-}C_5H_5)(C_4H_6)Cl_2]$ intra-C_4H_6 CH_2–CH 1.458(16) and 1.453(16) and CH–CH 1.375(16) Å.[40] The metallacyclopent-3-ene form of these complexes is also reflected in their ^1H and ^{13}C NMR spectra. In particular, the ^1J(C–H) coupling constants for the butadiene CH_2 groups are 10–25 Hz lower for σ^2,η^2-metallacyclopent-3-ene species compared to η^4-butadiene complexes,[40] reflecting the increased sp^3 hybridisation at these carbon centres for the former complexes.

In order to quantify the electronic character of $[M([9]aneS_3)(C_4H_6)]^+$ (M = Rh or Ir), ^1H-coupled ^{13}C NMR spectra of these complexes were obtained [90.56 MHz, $(CD_3)_2CO$, 293 K; Table 5). Using the semiempirical expression (1) relating

$$^1J(\text{C–H})/\text{Hz} = 5.70(\%\ \text{s}) - 18.4 \quad (1)$$

^1J(C–H) coupling constants to the degree of hybridisation at the C atom[49] we obtain a figure of 30.9% s character at the CH_2 centres of C_4H_6 in $[M([9]aneS_3)(C_4H_6)]^+$ (M = Rh or Ir). This corresponds to $n = 2.2$ for sp^n hybridisation at these C atoms. In contrast, metallacyclopent-3-ene species generally give $n = 2.6$–2.7 for these atoms.[40] Hence, the ^1J(C–H) coupling constants derived for $[M([9]aneS_3)(C_4H_6)]^+$ (M = Rh or Ir) are consistent with the $M(\eta^4\text{-}C_4H_6)$ structure generally observed for 1,3-diene complexes of the late transition metals such as $[M(CO)_3(C_4H_6)]$ (M = Fe, Ru or Os;[46] Table 5).

Other methods of analysing the bonding of diene fragments are based upon the distribution of bond lengths and dihedral angles in the diene fragment.[50] This approach defines two parameters Δd and Δl for a diene ligand labelled C(1), C(2), C(3) and C(4) (Fig. 5), equations (2) and (3). Using these guidelines,

$$\Delta d = 0.5\{d[\text{M–C(1)}] + d[\text{M–C(4)}]\} - 0.5\{d[\text{M–C(2)}] + d[\text{M–C(3)}]\} \quad (2)$$

$$\Delta l = 0.5\{d[\text{C(1)–C(2)}] + d[\text{C(3)–C(4)}]\} - d[\text{C(2)–C(3)}] \quad (3)$$

it has been observed that for σ^2,η^2-metallacyclopent-3-ene species Δd lies in the region −0.4 to 0 Å with Δl 0–0.2 Å. This compares with values of Δd = −0.1 to 0.1 Å and Δl −0.1 to 0 Å for η^4-butadiene complexes. In addition, the dihedral angle θ between the two planes defined by M–C(1)–C(4) and C(1)–C(2)–C(3)–C(4) is observed to fall in the region 75–90° for a η^4-butadiene complex and is >90° for the corresponding σ^2,η^2-metallacyclopent-3-ene species.[50] Based on the single-crystal structure analysis, the complex $[Ir([9]aneS_3)(C_4H_6)]^+$ has Δd = −0.012 Å, Δl = 0.066 Å and θ = 86.5°. Interestingly, Fryzuk *et al.*[51] have reported rather similar parameters for $[Ir(C_4H_6)\{N(SiMe_2CH_2PPh_2)_2\}]$ (Δd = −0.01 Å, Δl = 0.017 Å and θ = 92.9°). Based on the above criteria, the

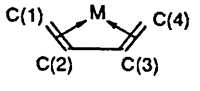

Fig. 5 Labelling of co-ordinated butadiene for bond length and angle analysis

Table 4 Bond lengths (Å), angles and torsion angles (°) with standard deviations for $[Ir([9]aneS_3)(C_4H_6)]^+$

Ir–S(1)	2.321(2)	C(3)–S(4)	1.828(10)
Ir–S(4)	2.331(2)	S(4)–C(5)	1.824(10)
Ir–S(7)	2.325(2)	C(5)–C(6)	1.517(13)
Ir–C(11)	2.149(9)	C(6)–S(7)	1.838(10)
Ir–C(12)	2.141(9)	S(7)–C(8)	1.837(9)
Ir–C(13)	2.146(9)	C(8)–C(9)	1.522(12)
Ir–C(14)	2.115(10)	C(11)–C(12)	1.433(13)
S(1)–C(2)	1.843(9)	C(12)–C(13)	1.381(13)
C(2)–C(3)	1.508(13)	C(13)–C(14)	1.461(14)
S(1)–Ir–S(4)	88.06(8)	C(2)–S(1)–C(9)	102.0(4)
S(1)–Ir–S(7)	88.87(8)	S(1)–C(2)–C(3)	111.5(6)
S(1)–Ir–C(11)	103.4(2)	C(2)–C(3)–S(4)	114.4(7)
S(1)–Ir–C(12)	142.0(2)	Ir–S(4)–C(3)	102.2(3)
S(1)–Ir–C(13)	144.3(2)	Ir–S(4)–C(5)	104.5(3)
S(1)–Ir–C(14)	105.0(3)	C(3)–S(4)–C(5)	100.7(4)
S(4)–Ir–S(7)	89.07(8)	S(4)–C(5)–C(6)	112.2(7)
S(4)–Ir–C(11)	168.0(2)	C(5)–C(6)–S(7)	113.4(7)
S(4)–Ir–C(12)	129.1(2)	Ir–S(7)–C(6)	101.5(3)
S(4)–Ir–C(13)	99.68(25)	Ir–S(7)–C(8)	105.4(3)
S(4)–Ir–C(14)	94.7(3)	C(6)–S(7)–C(8)	100.0(4)
S(7)–Ir–C(11)	94.86(25)	S(7)–C(8)–C(9)	111.9(6)
S(7)–Ir–C(12)	98.29(24)	S(1)–C(9)–C(8)	114.4(6)
S(7)–Ir–C(13)	125.7(2)	C(11)–C(12)–C(13)	119.1(8)
S(7)–Ir–C(14)	165.8(3)	C(12)–C(13)–C(14)	115.5(8)
Ir–S(1)–C(2)	106.1(3)		
Ir–S(1)–C(9)	102.2(3)		

S(1)–C(2)–C(3)–S(4)	−46.9(8)
C(2)–C(3)–S(4)–C(5)	−64.7(8)
C(3)–S(4)–C(5)–C(6)	136.1(7)
S(4)–C(5)–C(6)–S(7)	−50.2(8)
C(5)–C(6)–S(7)–C(8)	−65.4(7)
C(6)–S(7)–C(8)–C(9)	132.2(6)
S(7)–C(8)–C(9)–S(1)	−46.9(7)
C(8)–C(9)–S(1)–C(2)	−68.1(7)
C(9)–S(1)–C(2)–C(3)	132.9(6)
C(11)–C(12)–C(13)–C(14)	0.2(13)

Table 5 Carbon-13 NMR data for the butadiene ligand in metal–butadiene complexes

	δ [^1J(C–H)/Hz]		
Compound	CH_2 groups	CH groups	Ref.
$[Rh([9]aneS_3)(C_4H_6)]^+$	35.4 (158, 158)	90.0 (170)	20
$[Ir([9]aneS_3)(C_4H_6)]^+$	20.9 (156, 160)	79.5 (171)	This work
$[Fe(CO)_3(C_4H_6)]$	40.5 (158, 162)	85.5 (169)	46
$[Ru(CO)_3(C_4H_6)]$	32.7 (156, 160)	86.3 (168)	46
$[Os(CO)_3(C_4H_6)]$	24.2 (155, 160)	83.3 (170)	46
$[Fe(PMe_2Ph)_3(C_4H_6)]$	33.5 (154)	79.0 (163)	47
$[Zr(C_5H_5)_2(C_4H_6)]$	48.4 (145, 145)	110.9 (154)	39
$[Ta(C_5H_5)Cl_2(C_4H_6)]$	62.4 (146, 146)	126.1 (169)	40
Free C_4H_6	116.6 (158, 158)	137.2 (158)	48

complexes $[Ir([9]aneS_3)(C_4H_6)]^+$ and $[Ir(C_4H_6)\{N(SiMe_2CH_2PPh_2)_2\}]$ therefore appear to be approaching the cross-over between η^4-butadiene and σ^2,η^2-metallacyclopent-3-ene assignments. We therefore propose a structure for $[Ir([9]aneS_3)(C_4H_6)]^+$ involving predominantly η^4-butadiene co-ordination but with significant σ^2,η^2-metallacyclopent-3-ene contribution. The highly distorted intra-C_4H_6 C–C bond lengths observed in $[Ir([9]aneS_3)(C_4H_6)]^+$ probably arise from strong $C_4H_6 \rightarrow Ir$ σ donation consistent, as in $[Ir([9]aneS_3)(C_2H_4)_2]^+$, with the highly electrophilic nature of the cationic $[Ir([9]aneS_3)]^+$ fragment discussed above.

Cyclic voltammetry of all the above complexes in MeCN containing 0.1 mol dm^{-3} $NBu^n_4PF_6$ as base electrolyte shows irreversible oxidations at platinum electrodes at 298 K at a scan rate of 400 mV s^{-1}. Importantly, no reductive behaviour was observed, suggesting that these complexes are genuine iridium(I) rather than iridium(III) species. Coulometric measurements confirm the oxidations to be one-electron processes to give unknown diamagnetic species, possibly involving binuclear diiridium(II) species.

Experimental

Infrared spectra were run as KBr discs using a Perkin-Elmer 598 spectrometer over the range 200–4000 cm^{-1}, electronic spectra in 1 cm quartz cells using a Perkin-Elmer Lambda-9 spectrophotometer and FAB mass spectra on a Kratos MS 50TC spectrometer using a 3-nitrobenzyl alcohol matrix. Microanalyses were performed by the Edinburgh University Chemistry Department Microanalytical Service. Proton and ^{13}C NMR spectra were recorded at 200.13 and 50.32 MHz respectively on a Bruker WP200 spectrometer, and at 360.13 and 90.56 MHz on a Bruker WH360 spectrometer. 1,4,7-Trithiacyclononane was obtained from Aldrich Chemicals. The compounds $[Ir_2(C_8H_{14})_4Cl_2]$ and $[Ir_2(C_8H_{12})_2Cl_2]$ were synthesised according to literature methods.[16]

Syntheses.—$[Ir([9]aneS_3)(C_2H_4)_2]PF_6$. Ethene was bubbled through a solution of $[Ir_2(C_8H_{14})_4Cl_2]$ (0.075 g, 0.8 × 10^{-4} mol) in thf (6 cm^3) at 298 K for 10 min. To the resultant colourless solution was added $[9]aneS_3$ (0.030 g, 1.7 × 10^{-4} mol) and NH_4PF_6 (0.027 g, 1.7 × 10^{-4} mol), and the mixture was stirred at 293 K under N_2 for 15 min. The solution was filtered, and the solvent removed *in vacuo*. The crude product was recrystallised from CH_2Cl_2–hexane under N_2, and isolated as a pale yellow solid. Yield 0.048 g, 50% (Found: C, 20.7; H, 3.4. Calc. for $C_{10}H_{20}F_6IrPS_3$: C, 20.9; H, 3.5%). IR spectrum: 3040, 2990, 2920, 1470, 1450, 1435, 1410, 1300, 1285, 1265, 1225, 1190, 1170, 1130, 1015, 995, 970, 840, 740, 680, 660, 555, 490, 445 and 390 cm^{-1}. Electronic spectrum (MeCN): λ_{max} 229 (ε_{max} 8230), 290 (2350) and 356 nm (750 dm^3 mol^{-1} cm^{-1}). FAB mass spectrum: *m/z* 429 {calc. for $[^{193}Ir([9]aneS_3)(C_2H_4)_2]^+$ 429} 401 {calc. for $[^{193}Ir([9]aneS_3)(C_2H_4)]^+$ 401} and 373 {calc. for $[^{193}Ir([9]aneS_3)]^+$ 373}. NMR [$(CD_3)_2CO$, 293 K]: ^1H(360.13 MHz), δ 3.11–2.98 (m, $[9]aneS_3$, SCH_2, 12 H) and 2.19 (s, C_2H_4, 8 H); ^{13}C DEPT (50.32 MHz), δ 35.51 (s, $[9]aneS_3$, SCH_2) and 34.35 (s, C_2H_4).

$[Ir([9]aneS_3)(C_8H_{14})_2]PF_6$. The compounds $[Ir_2(C_8H_{14})_4Cl_2]$ (0.075 g, 0.8 × 10^{-4} mol), $[9]aneS_3$ (0.030 g, 1.7 × 10^{-4} mol) and NH_4PF_6 (0.027 g, 1.7 × 10^{-4} mol) were stirred in acetone (6 cm^3) under N_2 at 293 K for 15 min. The resultant pale yellow solution was filtered, reduced to *ca.* 1 cm^3, and the product crystallised with Et_2O. Recrystallisation from MeCN–Et_2O under N_2 yielded pale yellow microcrystals. Yield 0.081 g, 65% (Found: C, 35.6; H, 5.5. Calc. for $C_{22}H_{40}F_6IrPS_3$: C, 35.8; H, 5.5%). IR spectrum: 3000, 2970, 2910, 2860, 2670, 1465, 1450, 1435, 1410, 1355, 1340, 1320, 1285, 1260, 1240, 1225, 1205, 1190, 1175, 1145, 1120, 1090, 1070, 1040, 1020, 985, 975, 930, 905, 840, 740, 680, 660, 635, 605, 555, 540, 520, 485, 435 and 420 cm^{-1}. Electronic spectrum (MeCN): λ_{max} 245 (ε_{max} 8370), 285 (2300 dm^3 mol^{-1} cm^{-1}) and 335 (sh) nm. FAB mass spectrum: *m/z* 593 {calc. for $[^{193}Ir([9]aneS_3)(C_8H_{14})_2]^+$ 593}, 483 {calc. for $[^{193}Ir([9]aneS_3)(C_8H_{14})]^+$ 483} and 372 {calc. for $[^{193}Ir([9]aneS_3 - H)]^+$ 372}. NMR (CD_3NO_2, 293 K): ^1H(200.13 MHz), δ 5.62 (m, C_8H_{14} CH, 4 H) and 2.97–2.10 (m, $[9]aneS_3$ SCH_2 + C_8H_{14} CH_2, 36 H); ^{13}C DEPT (50.32 MHz), δ 61.44 (s, C_8H_{14}, CH), 35.19 (s, $[9]aneS_3$, SCH_2), 31.00, 28.41 and 25.02 (s, C_8H_{14}, CH_2).

$[Ir([9]aneS_3)(C_8H_{12})]PF_6$. Method as for $[Ir([9]aneS_3)(C_8H_{14})_2]PF_6$, using $[Ir_2(C_8H_{12})_2Cl_2]$ (0.056 g, 0.8 × 10^{-4} mol) in CH_2Cl_2 (6 cm^3). The product was a pale tan solid. Yield 0.035 g, 30% (Found: C, 26.7; H, 3.90. Calc. for $C_{14}H_{24}F_6IrPS_6$: C, 26.9; H, 3.9%). IR spectrum: 2980, 2940, 2910, 2870, 2820, 1470, 1445, 1410, 1370, 1330, 1300, 1260, 1245, 1210, 1170, 1155, 1140, 1120, 1075, 1025, 1010, 995, 965, 940, 920, 905, 875, 840, 780, 740, 705, 680, 660, 555, 525, 480, 450, 400 and 380 cm^{-1}. Electronic spectrum (MeCN): λ_{max} 249 (ε_{max} 15 300), 285 (2300 dm^3 mol^{-1} cm^{-1}) and 335 (sh) nm. FAB mass spectrum: *m/z* 625 {calc. for $[^{193}Ir([9]aneS_3 - H)(C_8H_{12})(PF_6)]^+$ 625}, 480 {calc. for $[^{193}Ir([9]aneS_3 - H)(C_8H_{12})]^+$ 480} and 372 {calc. for $[^{193}Ir([9]aneS_3 - H)]^+$ 372}. NMR (CD_3CN, 293 K): ^1H(200.13 MHz), δ 3.64 (m, C_8H_{12}, CH, 4 H), 2.84–2.54 (m, $[9]aneS_3$, SCH_2, 12 H), 2.32 and 2.12 (m, C_8H_{12}, CH_2, 4 H); ^{13}C DEPT (50.32 MHz), δ 63.03 (s, C_8H_{12}, CH), 35.53 (s, $[9]aneS_3$ SCH_2) and 32.27 (s, C_8H_{12} CH_2).

$[Ir([9]aneS_3)(C_4H_6)]PF_6$. Butadiene was bubbled through a CH_2Cl_2 (6 cm^3) solution of $[Ir_2(C_8H_{14})_4Cl_2]$ (0.075 g, 0.8 × 10^{-4} mol) for 5 min. The resultant colourless solution was then stirred with $[9]aneS_3$ (0.030 g, 1.7 × 10^{-4} mol) and NH_4PF_6 (0.027 g, 1.7 × 10^{-4} mol) under N_2 at 293 K for 30 min. The colourless solution was filtered, and the solvent removed *in vacuo*. The crude product was recrystallised from $MeNO_2$–Et_2O, giving a colourless microcrystalline solid. Yield 0.030 g, 25% (Found: C, 21.1; H, 3.1. Calc. for $C_{10}H_{18}F_6IrPS_3$: C, 21.0; H, 3.2%). IR spectrum: 3030, 2970, 2920, 1450, 1420, 1405, 1385, 1360, 1295, 1260, 1240, 1170, 1120, 1050, 1030, 1010, 980, 965, 940, 910, 875, 840, 740, 680, 660, 555, 500, 485, 460 and 405 cm^{-1}. Electronic spectrum (MeCN): λ_{max} 246 (ε_{max} 3900) and 278 nm (2270 dm^3 mol^{-1} cm^{-1}). FAB mass spectrum: *m/z* 427 {calc. for $[^{193}Ir([9]aneS_3)(C_4H_6)]^+$ 427}, 399 {calc. for $[^{193}Ir([9]aneS_3)(C_2H_2)]^+$ 399} and 372 {calc. for $[^{193}Ir([9]aneS_3 - H)]^+$ 372}. NMR [$(CD_3)_2CO$, 293 K]: ^1H(360.13 MHz), δ 5.29 (m, C_4H_6, CH, 2 H), 3.08–2.72 (m, $[9]aneS_3$, SCH_2, 12 H), 2.25 and 0.43 (m, C_4H_6, CH_2, 2 H); ^{13}C DEPT (90.56 MHz), δ 80.94 (s, C_4H_6, CH), 37.63, 36.46, 35.04 (s, $[9]aneS_3$, SCH_2) and 22.34 (s, C_4H_6, SCH_2).

Single-crystal Structure Determinations.—Single crystals of X-ray quality of $[Ir([9]aneS_3)(C_2H_4)_2]PF_6$, $[Ir([9]aneS_3)(C_8H_{12})]PF_6$ and $[Ir([9]aneS_3)(C_4H_6)]PF_6 \cdot 0.5Et_2O$ were obtained by diffusion of Et_2O vapour into acetone solutions of the complexes. Details of the crystal data, data collection and processing and structure analysis and refinement are given in Table 6. Low-temperature structure determinations were carried out using an Oxford Cryosystems low-temperature device.[53] All three structures were solved using a Patterson synthesis and developed by iterative cycles of least-squares refinement and Fourier difference syntheses.[54] Anisotropic thermal parameters were refined for all Ir, S, P and wholly occupied F and C atoms, and macrocyclic and {for $[Ir([9]aneS_3)(C_8H_{12})]PF_6$} C_8H_{12} H atoms were included in fixed, calculated positions.[53] Atomic coordinates appear in Tables 7–9. Illustrations were obtained using SHELXTL/PC,[55] and molecular geometry calculations utilised CALC.[56] Scattering-factor data were inlaid or taken from ref. 57. Individual details of structure refinement for each compound are now given.

$[Ir([9]aneS_3)(C_2H_4)_2]PF_6$. During refinement, the PF_6^- anion was found to be disordered over three equally occupied orientations by rotation about one F–P–F axis. The ethene H atoms could not be located, and were included in fixed positions so that C–H 1.08 Å, C–C–H 120° and Ir–C–C–H ± 103°.[54]

$[Ir([9]aneS_3)(C_8H_{12})]PF_6$. The macrocyclic C atoms were

Table 6 Experimental data for single-crystal X-ray structure determinations of $[Ir([9]aneS_3)L_2]PF_6$ *

L	C_2H_4	$0.5C_8H_{12}$	$0.5C_4H_6$
Formula	$C_{10}H_{20}F_6IrPS_3$	$C_{14}H_{24}F_6IrPS_3$	$C_{10}H_{18}F_6IrPS_3{\cdot}0.5C_4H_{10}O$
M_r	573.57	625.65	608.62
Crystal appearance	Yellow tablets	Yellow plates	Colourless tablets
Crystal dimensions/mm	0.70 × 0.39 × 0.12	0.29 × 0.08 × 0.03	0.47 × 0.35 × 0.23
Space group	$P2_1/n$	$P2_1/c$	$C2/c$
a/Å	11.461(3)	9.6404(8)	18.397(6)
b/Å	9.521(5)	11.9222(14)	8.593(4)
c/Å	15.653(8)	17.2174(18)	23.571(13)
β/°	105.44(4)	103.957(8)	97.79(3)
U/Å^3	1646	1921	3692
Z	4	4	8
D_c/g cm^{-3}	2.315	2.164	2.190
μ(Mo-Kα)/mm^{-1}	8.588	7.372	7.669
F(000)	1096	1208	2344
T/K	150	293	150
hkl ranges	−12 to 11, 0–10, 0–16	−10 to 10, 0–12, 0–18	−19 to 19, 0–9, 0–25
Data measured	3574	3709	2614
Data used [$F > 4\sigma(F)$]	2094	2372	2064
Absorption corrections			
ψ scans	No	Yes	Yes
Maximum and minimum corrections	—	0.4855, 0.3312	0.1585, 0.0954
DIFABS[52]	Yes	Yes	Yes
Maximum and minimum corrections	1.509, 0.799	1.144, 0.801	1.618, 0.760
Weighting scheme, w^{-1}	$\sigma^2(F) + 0.000\,11F^2$	$\sigma^2(F) + 0.000\,35F^2$	$\sigma^2(F) + 0.000\,14F^2$
Final R, R'	0.0278, 0.0360	0.0407, 0.0521	0.0315, 0.0405
Final S	1.099	1.162	1.059
Maximum and minimum residues in final ΔF synthesis/e Å^{-3}	0.88, −0.87	1.40, −0.78	0.95, −1.14

* Details in common: monoclinic; Stoë STADI-4 four-circle diffractometer; graphite-monochromated Mo-Kα radiation (λ = 0.710 73 Å); scan mode ω–2θ; $2\theta_{max}$ 45°.

Table 7 Atomic coordinates with estimated standard deviations (e.s.d.s) for $[Ir([9]aneS_3)(C_2H_4)_2]PF_6$

Atom	x	y	z
Ir	−0.067 720(20)	0.253 420(20)	0.140 390(20)
S(1)	0.092 60(14)	0.286 07(20)	0.264 94(12)
C(2)	0.139 7(6)	0.468 1(7)	0.263 1(5)
C(3)	0.110 9(6)	0.527 8(7)	0.170 8(5)
S(4)	−0.043 18(15)	0.494 96(18)	0.104 29(12)
C(5)	−0.131 3(6)	0.597 0(7)	0.165 4(5)
C(6)	−0.237 6(5)	0.512 6(7)	0.180 5(5)
S(7)	−0.197 20(13)	0.338 46(17)	0.225 42(11)
C(8)	−0.096 2(5)	0.381 1(7)	0.333 0(4)
C(9)	0.017 0(6)	0.289 6(8)	0.353 5(5)
C(11)	−0.232 6(6)	0.158 7(10)	0.059 3(5)
C(12)	−0.188 2(9)	0.244 7(9)	0.005 6(6)
C(13)	−0.002 7(7)	0.041 1(8)	0.149 3(5)
C(14)	0.051 1(6)	0.123 7(7)	0.092 5(5)
P	0.395 88(14)	0.316 33(19)	0.086 33(12)
F(1)	0.341 4(4)	0.288 1(5)	0.168 4(3)
F(2)	0.448 7(4)	0.345 0(5)	0.004 4(3)
F(3)	0.294 0(14)	0.240 5(18)	0.019 6(11)
F(4)	0.505 5(12)	0.410 1(20)	0.146 6(9)
F(5)	0.506 9(11)	0.211 7(16)	0.128 1(10)
F(6)	0.286 6(13)	0.420 2(19)	0.044 3(9)
F(7)	0.326 8(16)	0.469 7(15)	0.067 6(11)
F(8)	0.467 0(21)	0.176 5(19)	0.098 5(14)
F(9)	0.375 7(19)	0.145 6(16)	0.061 7(12)
F(10)	0.403 9(18)	0.469 0(13)	0.115 2(11)
F(11)	0.470 4(21)	0.449 3(17)	0.135 3(10)
F(12)	0.320 5(16)	0.180 8(21)	0.038 0(11)
F(13)	0.253 8(13)	0.342 2(21)	0.029 9(11)
F(14)	0.519 4(16)	0.277(3)	0.153 1(14)

Table 8 Atomic coordinates with e.s.d.s for $[Ir([9]aneS_3)(C_8H_{12})]PF_6$

Atom	x	y	z
Ir	0.174 91(5)	0.148 61(4)	0.181 76(3)
S(1)	0.139 9(5)	0.132 4(4)	0.044 31(24)
C(2)	0.110 4(23)	0.277 1(4)	0.008 9(4)
C(2′)	0.183(3)	0.269 9(7)	0.008 8(4)
C(3)	0.224 6(24)	0.352 3(7)	0.058 8(4)
C(3′)	0.136(3)	0.361 2(4)	0.058 9(4)
S(4)	0.222 5(5)	0.338 5(3)	0.164 4(3)
C(5)	0.412 7(7)	0.344 4(5)	0.213 2(12)
C(5′)	0.407 7(10)	0.342 8(6)	0.155 3(15)
C(6)	0.492 8(7)	0.258 3(4)	0.175 4(13)
C(6′)	0.496 0(6)	0.259 4(4)	0.213 3(15)
S(7)	0.425 6(4)	0.117 8(3)	0.189 0(3)
C(8)	0.409 6(12)	0.045 8(17)	0.093 5(6)
C(8′)	0.430 7(6)	0.108 0(21)	0.083 7(3)
C(9)	0.318 8(6)	0.115 8(21)	0.026 8(3)
C(9′)	0.296 4(12)	0.049 8(17)	0.037 3(6)
C(11)	0.222 2(15)	0.149 6(11)	0.311 1(8)
C(12)	0.088 5(14)	0.202 0(11)	0.283 2(8)
C(13)	−0.053 1(15)	0.146 8(12)	0.286 4(9)
C(14)	−0.120 4(15)	0.092 9(16)	0.209 8(10)
C(15)	−0.019 6(15)	0.047 8(13)	0.164 5(8)
C(16)	0.102 4(16)	−0.017 1(11)	0.199 2(9)
C(17)	0.147 0(15)	−0.052 9(12)	0.289 2(9)
C(18)	0.243 0(16)	0.032 2(12)	0.342 9(9)
P	0.659 6(4)	0.213 7(3)	0.456 09(23)
F(1)	0.618 8(17)	0.131 2(11)	0.386 0(10)
F(2)	0.757 6(15)	0.281 5(11)	0.415 2(10)
F(3)	0.787 1(13)	0.135 4(9)	0.494 6(10)
F(4)	0.555 8(15)	0.148 2(11)	0.496 2(10)
F(5)	0.528 1(11)	0.289 2(11)	0.418 2(8)
F(6)	0.691 4(15)	0.299 8(13)	0.525 8(8)

found to be disordered over two equally occupied orientations. This disorder was modelled using the fixed parameters C–C 1.52, S–C 1.83 Å, S–C–C 109°.

$[Ir([9]aneS_3)(C_4H_6)]PF_6{\cdot}0.5Et_2O$. The Et_2O solvent molecule was located across a crystallographic two-fold axis, and was observed to be disordered over two distinct orientations. The C_4H_6 H atom positions were allowed to refine with fixed C–H 1.08 Å and using free variables so that all C–C–H and H–C–H angles were constrained to be equal.[54]

Table 9 Atomic coordinates with e.s.d.s for $[Ir([9]aneS_3)(C_4H_6)]PF_6 \cdot 0.5Et_2O$

Atom	x	y	z
Ir	0.405 360(20)	0.231 65(3)	0.074 380(10)
S(1)	0.408 15(13)	0.194 1(3)	0.172 59(11)
C(2)	0.415 6(5)	−0.016 2(10)	0.182 1(4)
C(3)	0.456 7(5)	−0.092 1(10)	0.137 8(5)
S(4)	0.422 36(12)	−0.034 38(24)	0.063 93(11)
C(5)	0.330 0(4)	−0.119 7(9)	0.056 9(4)
C(6)	0.271 5(4)	−0.004 5(8)	0.031 7(4)
S(7)	0.279 72(11)	0.188 94(22)	0.064 42(9)
C(8)	0.257 6(5)	0.149 6(10)	0.137 0(4)
C(9)	0.312 2(6)	0.224 8(10)	0.182 2(4)
C(11)	0.424 8(5)	0.289 1(10)	−0.011 0(4)
C(12)	0.490 6(4)	0.311 8(10)	0.028 2(4)
C(13)	0.488 7(5)	0.406 7(9)	0.075 3(4)
C(14)	0.417 5(6)	0.476 1(9)	0.080 6(5)
P	0.320 06(14)	0.132 4(3)	0.359 80(11)
F(1)	0.248 9(3)	0.070 6(7)	0.384 5(3)
F(2)	0.303 9(4)	0.017 4(6)	0.306 16(25)
F(3)	0.391 2(3)	0.193 3(8)	0.334 9(3)
F(4)	0.334 8(4)	0.248 3(7)	0.412 8(3)
F(5)	0.272 0(4)	0.262 2(6)	0.324 7(3)
F(6)	0.369 1(4)	0.006 1(8)	0.395 0(3)
O(1S)	0.0000	0.143 7(10)	0.250 0
C(1S)	0.051 9(12)	0.054 9(23)	0.226 0(10)
C(2S)	0.063 6(16)	0.069(3)	0.248 8(12)
C(3S)	0.129 8(11)	0.119 2(22)	0.241 3(10)
C(4S)	0.111 5(12)	0.147 3(22)	0.212 1(10)

Additional material available from the Cambridge Crystallographic Data Centre comprises H-atom coordinates, thermal parameters and remaining bond lengths and angles.

Acknowledgements

We thank the SERC and ICI Colours and Fine Chemicals (Blackley) for a CASE award (to M. A. H.), Johnson-Matthey plc for generous loans of platinum metal salts, and the Royal Society of Edinburgh and Scottish Office Education Department for a Support Research Fellowship (to M. S.).

References

1 R. Cramer, *J. Am. Chem. Soc.*, 1964, **86**, 217; R. Cramer, J. B. Kline and J. D. Roberts, *J. Am. Chem. Soc.*, 1969, **91**, 2519; R. Cramer and L. J. Guggenberger, *J. Am. Chem. Soc.*, 1972, **94**, 3779; R. Cramer, *J. Am. Chem. Soc.*, 1972, **94**, 5681.

2 W. A. G. Graham, *J. Organomet. Chem.*, 1986, **300**, 81 and refs. therein; A. J. Rest, I. Whitwell, W. A. G. Graham, J. K. Hoyano and A. D. McMaster, *J. Chem. Soc., Dalton Trans.*, 1987, 1181; S. T. Belt, S. B. Duckett, D. M. Haddleton and R. N. Perutz, *Organometallics*, 1988, **7**, 1526; *Organometallics*, 1989, **8**, 748; D. M. Haddleton, A. McCamley and R. N. Perutz, *J. Am. Chem. Soc.*, 1988, **110**, 1810; T. W. Bell, D. M. Haddleton, A. McCamley, M. G. Partridge, R. N. Perutz and H. Willner, *J. Am. Chem. Soc.*, 1990, **112**, 9212; T. W. Bell, S.-A. Brough, M. C. Partridge, R. N. Perutz and A. D. Rooney, *Organometallics*, 1993, **12**, 2933.

3 W. D. Jones and F. J. Feher, *Acc. Chem. Res.*, 1989, **22**, 91; R. G. Bergman, *J. Organomet. Chem.*, 1990, **400**, 273.

4 C. K. Ghosh and W. A. G. Graham, *J. Am. Chem. Soc.*, 1987, **109**, 4726; 1989, **111**, 375.

5 M. J. Fernandez, M. J. Rodriguez, L. A. Oro and F. J. Lahoz, *J. Chem. Soc., Dalton Trans.*, 1989, 2073; R. S. Tanke and R. H. Crabtree, *Inorg. Chem.*, 1989, **28**, 3444; O. Boutry, E. Gutierrez, A. Monge, M. C. Nicasio, P. J. Perez and E. Carmona, *J. Am. Chem. Soc.*, 1992, **114**, 7288; P. J. Perez, M. L. Poveda and E. Carmona, *J. Chem. Soc., Chem. Commun.*, 1992, **8**, 558.

6 C. Bianchini, E. Farnetti, M. Graziani, G. Nardin, A. Vacca and F. Zanobini, *J. Am. Chem. Soc.*, 1990, **112**, 9190; C. Bianchini, A. Meli, M. Perruzzini, F. Vizza, P. Frediani and J. Ramirez, *Organometallics*, 1990, **9**, 226; D. J. Rauscher, E. G. Thaler, J. C. Huffman and K. G. Caulton, *Organometallics*, 1991, **10**, 2209; P. Barbaro, C. Bianchini, A. Meli, M. Perruzzini, A. Vacca and F. Vizza, *Organometallics*, 1991, **10**, 2227; C. Bianchini, K. G. Caulton, K. Folting, A. Meli, M. Peruzzini, A. Polo and F. Vizza, *J. Am. Chem. Soc.*, 1992, **114**, 7290; C. Bianchini, P. Frediani, M. Graziani, J. Kasper, A. Meli, M. Peruzzini and F. Vizza, *Organometallics*, 1993, **12**, 2886.

7 C. J. Besecker, V. W. Day and W. G. Klemperer, *Organometallics*, 1985, **4**, 564; V. W. Day, W. G. Klemperer, S. P. Lockledge and D. J. Main, *J. Am. Chem. Soc.*, 1990, **112**, 2031.

8 R. S. Tanke and R. H. Crabtree, *J. Am. Chem. Soc.*, 1990, **112**, 7984.

9 M. Schröder, *Pure Appl. Chem.*, 1988, **60**, 517; S. R. Cooper, *Acc. Chem. Res.*, 1988, **21**, 141; S. R. Cooper and S. C. Rawle, *Struct. Bonding (Berlin)*, 1990, **72**, 1; A. J. Blake and M. Schröder, *Adv. Inorg. Chem.*, 1990, **35**, 1 and refs. therein.

10 See, for example, W. N. Setzer, C. A. Ogle, G. S. Wilson and R. S. Glass, *Inorg. Chem.*, 1983, **22**, 266; S. C. Rawle, T. J. Sewell and S. R. Cooper, *Inorg. Chem.*, 1987, **26**, 3769; H.-J. Küppers, K. Wieghardt, Y.-H. Tsay, C. Krüger, B. Nuber and J. Weiss, *Angew. Chem., Int. Ed. Engl.*, 1987, **26**, 575; A. J. Blake, A. J. Holder, T. I. Hyde and M. Schröder, *J. Chem. Soc., Chem. Commun.*, 1987, 987; *J. Chem. Soc., Dalton Trans.*, 1988, 1861; A. J. Blake, A. J. Holder, T. I. Hyde, G. Reid and M. Schröder, *Polyhedron*, 1989, **8**, 2041.

11 A. J. Blake, R. O. Gould, A. J. Holder, T. I. Hyde, G. Reid and M. Schröder, *J. Chem. Soc., Dalton Trans.*, 1990, 1759.

12 J. Chatt, G. J. Leigh, A. P. Storace, D. A. Squire and B. J. Starkey, *J. Chem. Soc. A*, 1971, 899.

13 A. J. Blake, R. O. Gould, G. Reid and M. Schröder, *J. Organomet. Chem.*, 1988, **356**, 389.

14 For example, K. Wieghardt, H.-J. Küppers, E. Raabe and C. Krüger, *Angew. Chem., Int. Ed. Engl.*, 1986, **25**, 1101; A. J. Blake, A. J. Holder, T. I. Hyde, Y. V. Roberts, A. J. Lavery and M. Schröder, *J. Organomet. Chem.*, 1987, **323**, 261; A. J. Blake, R. O. Gould, A. J. Holder, T. I. Hyde, M. O. Odulate, A. J. Lavery and M. Schröder, *J. Chem. Soc., Chem. Commun.*, 1987, 118; A. J. Blake, R. O. Gould, J. A. Greig, A. J. Holder, T. I. Hyde and M. Schröder, *J. Chem. Soc., Chem. Commun.*, 1989, 876.

15 A. J. Blake, M. A. Halcrow and M. Schröder, *J. Chem. Soc., Chem. Commun.*, 1991, 253.

16 J. L. Herde, J. C. Lambert and C. V. Senoff, *Inorg. Synth.*, 1974, **15**, 18.

17 A. Van der Ent and T. C. Van Soest, *Chem. Commun.*, 1970, 225.

18 A. L. Onderlinden and A. Van der Ent, *Inorg. Chim. Acta*, 1972, **6**, 420.

19 M. A. Halcrow, Y. V. Roberts and M. Schröder, unpublished work.

20 A. J. Blake, R. O. Gould, M. A. Halcrow and M. Schröder, *J. Chem. Soc., Dalton Trans.*, in the press.

21 R. Cramer and J. J. Mrowca, *Inorg. Chim. Acta*, 1971, **5**, 528.

22 H. Eshtiagh-Hosseini and J. F. Nixon, *J. Less-Common Met.*, 1978, **61**, 107; M. Mlekuz, P. Bougeard, B. G. Sayer, M. J. McGlinchey, C. A. Rodger, M. J. Churchill, J. W. Ziller, S.-K. Kang and T. A. Albright, *Organometallics*, 1986, **5**, 1656.

23 K. Moseley, J. W. Kang and P. M. Maitlis, *J. Chem. Soc. A*, 1970, 2875.

24 M. A. Bennett and T. W. Matheson, *J. Organomet. Chem.*, 1978, **153**, C25.

25 J. A. Segal and B. F. G. Johnson, *J. Chem. Soc., Dalton Trans.*, 1975, 677.

26 C. E. Holloway, G. Hulley, B. F. G. Johnson and J. Lewis, *J. Chem. Soc. A*, 1970, 1653.

27 N. C. Harrison, M. Murray, J. L. Spencer and F. G. A. Stone, *J. Chem. Soc., Dalton Trans.*, 1978, 1337.

28 A. J. Blake, A. J. Holder, T. I. Hyde and M. Schröder, *J. Chem. Soc., Chem. Commun.*, 1989, 1433.

29 D. P. Riley and J. D. Oliver, *Inorg. Chem.*, 1983, **22**, 3361.

30 E. G. Lundquist, K. Folting, W. E. Streib, J. C. Huffman, O. Eisenstein and K. G. Caulton, *J. Am. Chem. Soc.*, 1990, **112**, 855; C. Chardon, O. Eisenstein, T. Johnson and K. G. Caulton, *New J. Chem.*, 1992, **16**, 781.

31 R. J. Restivo, G. Ferguson, T. L. Kelly and C. V. Senoff, *J. Organomet. Chem.*, 1975, **90**, 101.

32 A. R. Rossi and R. Hoffman, *Inorg. Chem.*, 1975, **14**, 365.

33 M. R. Churchill and S. A. Bezman, *Inorg. Chem.*, 1972, **11**, 2243; 1973, **12**, 260, 531.

34 R. P. Hughes, N. Krishnamachari, C. J. L. Lock, J. Powell and G. Turner, *Inorg. Chem.*, 1977, **16**, 314.

35 L. Kruczinsky and J. Takats, *J. Am. Chem. Soc.*, 1974, **96**, 932; *Inorg. Chem.*, 1976, **15**, 3140; M. A. Busch and R. J. Clark, *Inorg. Chem.*, 1975, **14**, 226; A. D. English, J. P. Jesson and C. A. Tolman, *Inorg. Chem.*, 1976, **15**, 1730.

36 T. A. Albright, P. Hofmann and R. Hoffmann, *J. Am. Chem. Soc.*, 1977, **99**, 7546.
37 G. Erker, J. Wicher, K. Engel and C. Krüger, *Chem. Ber.*, 1982, **115**, 3300; G. Erker, K. Engel, C. Krüger and A.-P. Chiang, *Chem. Ber.*, 1982, **115**, 3311.
38 G. Erker, K. Engel, C. Krüger and G. Müller, *Organometallics*, 1984, **3**, 128.
39 Y. Kai, N. Kaneshi, K. Miki, N. Kasai, M. Akita, H. Yasuda and A. Nakamura, *Bull. Chem. Soc. Jpn.*, 1983, **56**, 3735.
40 H. Yasuda, K. Tatsumi, T. Okamoto, K. Mashima, K. Lee, A. Nakamura, Y. Kai, N. Kaneshi and N. Kawai, *J. Am. Chem. Soc.*, 1985, **107**, 2410; Ch. Elschenbroich and A. Salzer, *Organometallics, A Concise Introduction*, VCH, Weinheim, 1989.
41 O. S. Mills and G. Robinson, *Acta Crystallogr.*, 1963, **16**, 758.
42 L. C. A. de Carvahlo, Y. Peres, M. Dartiguenave, Y. Dartiguenave and A. L. Beauchamp, *Organometallics*, 1985, **4**, 2021.
43 W. Haugen and M. Traettenberg, *Acta Chem. Scand.*, 1966, **20**, 1726.
44 D. M. P. Mingos, in *Comprehensive Organometallic Chemistry*, eds. G. Wilkinson, F. G. A. Stone and E. Abel, Pergamon, Oxford, 1982, vol. 3, ch. 11, pp. 60–67 and refs. therein; F. A. Cotton, V. W. Day, B. A. Frenz, K. I. Hardcastle and J. M. Troup, *J. Am. Chem. Soc.*, 1973, **95**, 4522.
45 T. C. Van Soest, A. Van der Ent and E. C. Royers, *Cryst. Struct. Commun.*, 1973, **2**, 527; A. Immirzi and G. Allegra, *Acta Crystallogr., Sect. B*, 1969, **25**, 120.
46 S. Ruh and W. von Philipsborn, *J. Organomet. Chem.*, 1977, **127**, C59; S. Zobl-Ruh and W. von Philipsborn, *Helv. Chim. Acta*, 1980, **63**, 773.
47 S. Komiya, H. Minato, T. Ikariya, T. Yamamoto and A. Yamamoto, *J. Organomet. Chem.*, 1983, **254**, 83.
48 H. L. Retcofsky, E. N. Frankel and H. S. Gutowsky, *J. Am. Chem. Soc.*, 1966, **88**, 2710.
49 M. D. Newton, J. M. Schulman and M. M. Manus, *J. Am. Chem. Soc.*, 1974, **96**, 17.
50 H. Yasuda and A. Nakamura, *Angew. Chem., Int. Ed. Engl.*, 1987, **26**, 723.
51 M. D. Fryzuk, K. Joshi and S. J. Rettig, *Polyhedron*, 1989, **8**, 2291.
52 DIFABS, Program for Empirical Absorption Corrections, N. Walker and D. Stuart, *Acta Crystallogr., Sect. A*, 1983, **39**, 158.
53 J. Cosier and A. M. Glazer, *J. Appl. Crystallogr.*, 1986, **19**, 105.
54 SHELX 76, Program for Crystal Structure Determination, G. M. Sheldrick, University of Cambridge, 1976.
55 SHELXTL/PC version 4.2, G. M. Sheldrick, University of Göttingen, 1989 (Siemens Analytical X-Ray Instrumentation, Madison, WI).
56 CALC, Fortan 77 version, R. O. Gould and P. Taylor, University of Edinburgh, 1985.
57 D. T. Cromer and J. B. Mann, *Acta Crystallogr., Sect. A*, 1968, **24**, 321.

Received 20*th January* 1994; *Paper* 4/00371C